# A ROBUST TECHNIQUE FOR TRACKING PARTICLES OVER LONG IMAGE SEQUENCES

Frank Hering, Michael Merle, Dietmar Wierzimok[1]
Institute for Environmental Physics, University of Heidelberg
Im Neuenheimer Feld 366,D-69120 Heidelberg, Germany
Phone: (49) 06221-563403, email: fhering@dali.uphys.uni-heidelberg.de
[1] Now affiliated to IBM Research Center Heidelberg, FRG.

Bernd Jähne
Interdisciplinary Center for Scientific Computing
University of Heidelberg, Im Neuenheimer Feld 368, D-69120 Heidelberg, Germany
and
Scripps Institution of Oceanography
Physical Oceanography Research Division, University of California
La Jolla, CA 92093-0230, USA

KEY WORDS: Particle Tracking Velocimetry, Flow Visualization, Correspondence Problem

## ABSTRACT:

A particle tracking technique at high particle concentration for the evaluation of flow fields beneath water waves is described. A 1-4 cm thick light sheet parallel to the main wave propagation direction was used to illuminate small polystyrol seeding particles. The depth of the light sheet was chosen such that the particles stay long enough in the illuminated area to enable tracking. An area of up to $14.0 \times 9.0\,cm^2$ is observed by a digital CCD camera. The recording of continuous image sequences at up to 60 fields/s allow an extensive study of the flow field. An automatic tracking algorithm is described allowing particles to be followed over more than 200 images at particle concentrations up to 800 particles/image (image resolution $480 \times 512$ pixel), yielding both Lagrangian and Eulerian vector field. The error of the computation of a velocity vector is usually below 3 %.

## 1 INTRODUCTION

Most particle tracking techniques use streak photography [7] as a tool for the determination of the flow field. The velocity field can be obtained by measuring length, orientation and location of each streak [4]. The length is commonly calculated from the end points of a streak, detected by a segmentation algorithm. This approach to particle tracking is only feasible at low particle concentration up to typically 30-100 particles/image [4] [1]. Most authors use a physical model as an interpolation scheme for identifying the same particle in the next image frame [1] [3]. This paper describes a novel particle tracking algorithm, allowing to track up to 800 particles/frame using the image field overlap as the primary feature for solving the correspondence problem.

## 2 OPTICAL SET-UP

A 1-4 cm thick light sheet parallel to the main wave propagation direction is used to illuminate small LATEX seeding particles. The light sheet is typically generated from beneath of the channel by Halogen lamps (see Fig. 1). The visualization used in Delft and in Heidelberg are basically identical and have been described earlier by [12] and [11]. An area of typically $14.0 \times 9.0\,cm^2$ is imaged by a 60 Hz CCD camera (Pulnix TM-740 and Sony XC75) with a spatial resolution Due to the movement of the particles during the exposure time, they are imaged as streaks (Fig. 2). The image sequences are stored on a Laser Video Disc (Sony LVR 5000) for later evaluation.


doi: 10.5281/zenodo.14890

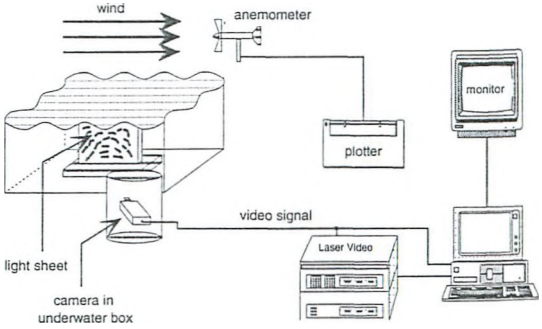


Figure 1: *Scheme of the optical instruments used at linear flume in Delft: A camera in an underwater box is looking perpendicular on a light sheet, illuminating seeding particles.*

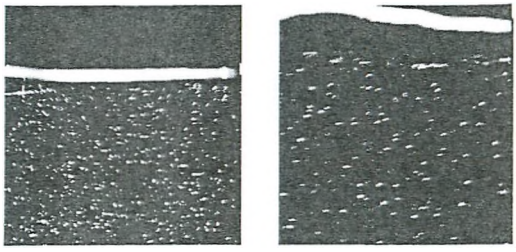

Figure 2: *Seeding particles at a wind speed of 4.2 m/s (left) and 6.4 m/s (right) beneath the water surface in a light sheet illumination. Due to the exposure time of the camera particles in motion are visualized as streaks.*

## 3 DETERMINATION OF THE 2-D FLOW VECTOR FIELD

Several steps of image processing are required for the extraction of the flow field from the image sequences. After the digitization of each picture is parted into its two image fields. A specially developed segmentation technique for identifying individual particles from the background follows. Each object is labeled and finally the correspondence problem of identifying the same object in the next image frame is solved by calculating its streak overlap. Repeating this algorithm will track segmented particles through the image sequence.

### 3.1 Preprocessing

An image taken with a standard CCD camera at a frequency of 30 Hz (NTSC-norm) actually consists of two consecutive fields of only half vertical resolution. Therefore it is required to split the original gray value image g(x,y) into its two fields; one field $g_1(x,y)$ being the odd and the second field $g_2(x,y)$ being the even rows of g(x,y).

### 3.2 Segmentation

The histogram (Fig. 3) of a streak image shows two distinct maxima, at the low gray values being faint particle streaks and the background and at high gray values being reflections at the water surface and bright particles. Therefore the intensity of the streaks ranges from the very low to the very high gray value. Simple pixel based segmentation techniques cannot be chosen as the streak images do not show a true bimodal distribution in the histogram. A region growing algorithm was developed for the discrimination of individual particles from the background. Regions with similar features are to be identified and merged together to a

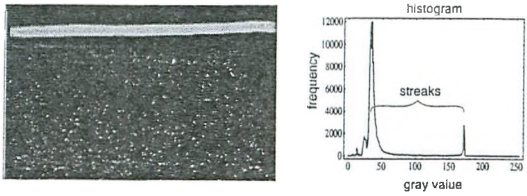


Figure 3: *Histogram of the left streak image. Although appearing to show a bimodal distribution, particles cannot be segmented by a threshold.*

connected object. The image g(x,y) is scanned through for local maxima in the intensity, as the location of streaks is well approximated by a local maximum $g_{max}(x,y)$. A minimum search horizontally and vertically from $g_{max}(x,y)$ enables the calculation of the peak height:

$$\Delta g \quad = \quad \min(g_{max} - g_{min,i}) \; , \tag{1}$$

$g_{min,i}$ being the minima revealed by the minimum search. In addition the half width is measured. Both peak height and half width a required to lie above a threshold to prevent random noise being a seeding point for the region growing. After these germ points are identified the growing algorithm segments the object following two rules: A pixel is accepted as an object point only when its gray value is higher than an adaptive threshold, which is calculated from $g_{min,i}$ by interpolation. Then,only those pixels forming a connected object are considered. A result of the described segmentation algorithm is shown in Fig. 4. Each object identified by the segmentation is then labeled with a flood fill algorithm borrowed from computer graphics. The size of each object can then be determined, and thereby large objects (reflections at the water surface) removed.

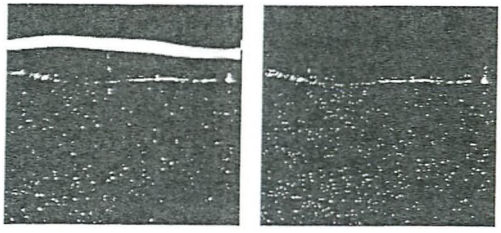

Figure 4: *Original gray value image left and segmented image right. 501 objects were found. The reflections at the water surface were eliminated by the labeling algorithm.*

## 3.3 Image Sequence Analysis

After segmentation, the correspondence problem of identifying the same particle in the next image frame is solved, by calculating its image field streak overlap: Some cameras (e.g. the Pulnix TM-640) show a significant overlap $\theta$ of the exposure in two consecutive fields of the same frame. The overlap of the exposure time yields a spatial overlap of the two corresponding streaks from one image to the next. An AND operation between two consecutive segmented fields calculates the overlap fast and efficiently [6]. In addition, as the temporal order of the image fields is known, the sign of the vector is also known and the directional ambiguity is removed. However most cameras do not show a temporal overlap in the exposure time. then, corresponding particles will only overlap due to their expansion in space. Artificially this expansion can be increased by the use of a morphological dilation operator. The binary dilation operator of the set of object points $\mathcal{O}$ by a mask M is defined by:

$$\mathcal{O} \oplus M = \{p : \; M_p \cap \mathcal{O} \neq \emptyset\} \; , \tag{2}$$

where $M_p$ denotes the shift of the mask to the point p, in that way that p is localized at the reference point of the mask. The dilation of $\mathcal{O}$ by the mask M is therefore the set of all points, where the intersecting set of $\mathcal{O}$ and $M_p$ is not empty. This operation will enlarge objects and typically smooth their border. For more details see [8]. To avoid unnecessary clustering of the objects the dilation is not calculated simultaneously for all objects in an image but for each object individually [9]. In most cases, in particular for low particle concentration($\leq$ 300 particles/image), each particle shows only the overlap with corresponding particle in the next frame. At higher particle concentration, particles however show overlap with up to typically four particles in the next frame. Therefore additional features are required to minimize false correspondences. Ideally the sum of gray value for each streak in the image series should be constant, due to the equation of continuity for gray values [6]:

$$\sum_{x,y \in \mathcal{O}} g(x,y) \; = \; const. \, . \tag{3}$$

This implies a particle at low speed is visualized as a small bright spot. The same particle at higher speed is imaged as a fainter object extending over a larger area. The sum of gray value in both cases should be identical. The sum of gray value however is erroneous to compute due to ever present segmentation errors. Therefore it is more convenient to normalize the sum of gray value by the occupied area. The normalized sum of gray value being $G_n^1$ of the first frame and $G_n^2$ of the second are required to lie above a threshold of the confidence interval C:

$$C \;\; = \;\; 1 - \frac{|G_n^1 - G_n^2|}{|G_n^1 + G_n^2|} \;\; \longmapsto \;\; [0,1] \, . \tag{4}$$

A similar expression can be derived for the area of the objects.

### 3.4 Calculation of the displacement vector field

*Wierzimok* and *Hering* [11] showed that the center of gray value $\vec{x}_c$ of an isotropic object represents the timely averaged two dimensional location $\langle \vec{x} \rangle_{\Delta t}$, thus:

$$\vec{x}_c = \langle \vec{x} \rangle_{\Delta t} \, . \tag{5}$$

Now the knowledge of the location of the same particle in the previous frame (at the time $t-1$) enables the first-order approximation the velocity field $\vec{u}(t)$:

$$\vec{u}(t) \approx \frac{\vec{x}_c(t) - \vec{x}_c(t-1)}{\Delta t} \tag{6}$$

Repeating the described algorithm will automatically track all encountered seeding particles from one frame to the next.

## 4 CALIBRATION AND TESTS OF THE PARTICLE TRACKING ALGORITHM

The calibration technique is the same as described earlier by [12]. A calibration grid centered in the light sheet is used to calibrate the image coordinate system. The grid points provide points of known location in both world an the image coordinate system. Therefore the coefficients of the image transformation can be reconstructed. algorithms have been implemented on an i860 board to achieve maximum performance. Typical evaluation time of one image including digitization, segmentation and tracking is 10 s. Long image sequences (200-1000) images can therefore be processed. Individual particles can be tracked up to a concentration of 800 particles/image at an image size of $480 \times 512$ pixel.

For testing the efficiency of the algorithms small particles were attached to a rotating disc of a LP-player [9]. The disc rotated at constant frequency of 33 rpm, see Fig. 5. As therefore each vector of a trajectory has the same absolute velocity, one can calculate the standard error $\sigma_{\overline{v}}$ for the determination of a displacement vector by:

$$\sigma_{\overline{v}} \;\; = \;\; \sqrt{\frac{\sum_{i=1}^{N} (\overline{v_i} - ||\vec{v}_i||)^2}{N(N-1)}} \, , \tag{7}$$

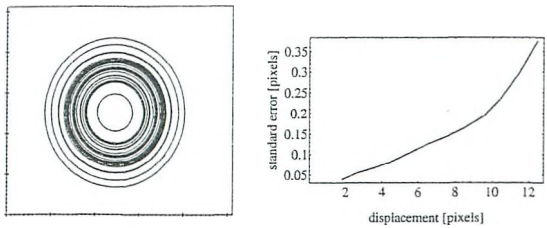


Figure 5: *Trajectories of particles attached to disc at 33 rpm (left).Standard error for the calculation of displacement vectors (right).*

$\overline{v_i}$ being the mean displacement, $||\vec{v}_i||$ the i-th displacement in the trajectory and N the number of displacement vectors in the trajectory. Fig. 5 shows the standard error for displacement vectors up to 12 pixels per frame, calculated from more than 100000 vectors. The error always stays well below 3%.

## 5 PARTICLE TRACKING BENEATH WATER WAVES

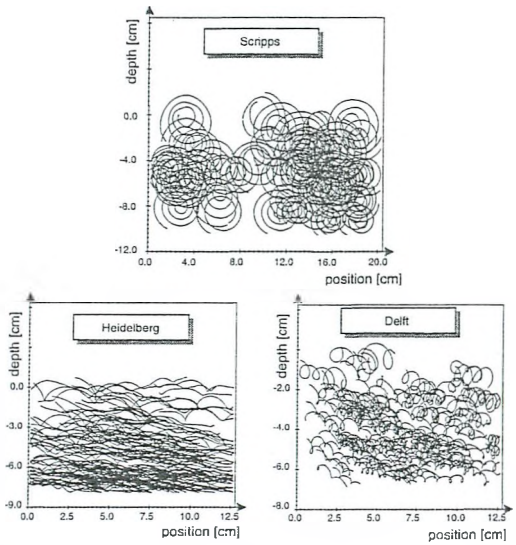


Figure 6: *Trajectories of seeding particles beneath mechanically generated waves (top) and wind induced water waves (bottom).*

Fig. 6 shows three typical trajectories measured at circular wind/wave facility in Heidelberg and at the linear flumes in Delft and Scripps. Particle concentration in Heidelberg is about 800 particles/image, about 250 particles/image in Delft and 600 particles/image in Scripps. The concentration in Delft is lower due to the more difficult visualization involved. In both cases 100 images were processed. For presentation only a fraction of the trajectories were plotted. Only trajectories tracked over 90 image frames(3 s) were considered. Many particles can be tracked from the moment entering into the light sheet until leaving the

area of observation. The information from the particle tracking is used for the study of mass transport [11] and the interaction of waves [5].

## 6 CONCLUSIONS AND OUTLOOK

A powerful particle tracking algorithm was described, enabling to track particles over several wave periods at particle concentration up to 800 particles per image. Particle tracking for the first time, enters the domain of digital particle image velocimetry as described by [4]. In addition PTV yields both the Eulerian and Lagrangian flow field. This technique als allows an easy extension to the 3rd dimension, which is currently undertaken in cooperation with the BASF [10], by directly correlating the trajectories imaged from different camera perspectives.

## ACKNOWLEDGEMENTS

Financial support for this research from the National Science Foundation (OCE91 15994) and the German Science Foundation DFG (Wi1029/2-1) is gratefully acknowledged.

## REFERENCES

[1] Adamczyk, A.A., Rimai, L.: 1988, '2-Dimensional Particle Tracking Velocimetry (PTV): Technique and image processing algorithm', *Experiments in Fluids 6, Springer-Verlag, 373-380*

[2] Adrian, R.J.: 1991, 'Particle-Imaging Techniques for Experimental Fluid Mechanics', *Ann. Rev. Fluid Mech., 23, 261-304*

[3] Etoh, T., Takehara, K.: 1992, 'An Algorithm for Tracking Particles', *Proceedings, 6th International Symposium on Stochastic Hydraulics, Tapei, 237-241*

[4] Gharib, M., Willert, C.: 1988, 'Particle Tracing Revisited', *Proceedings, 1st National Fluid Dynamics Congress, Cincinnati/Ohio, AIAA-88-3776-CP,*

[5] Hering, F., Wierzimok, D., Melville, W.K., Jähne, B.: 1993, 'Combined Wave and Flow Field Visualization for the Investigation of Short-Wave/Long-Wave Interaction', *Proceedings, Air-Sea Interface Symposium, Marseille 24.-30. June , in print*

[6] Hering, F.: 1992, 'Messung von Transportgeschwindigkeiten in winderzeugten Wasserwellen mittels Digitaler Bildfolgenanalyse', *Diploma thesis, Institute for Environmental Physics, University of Heidelberg*

[7] Hesselink, L.: 1988, 'Digital image processing in flow visualization', *Ann. Rev. Fluid Mech, 20, 421-485*

[8] Jähne, B.: 1993, 'Digital Image Processing', *Concepts, Algorithms and Scientific Applications, 2nd edition, Springer-Verlag, Berlin, 200-205*

[9] Merle, M.: 1993, 'Genauigkeit von Particle Tracking Velocimetry', *Diploma thesis, Institute for Environmental Physics, University of Heidelberg*

[10] Netzsch, T., Jähne, B.: 1994, 'A high performance for 3-dimensional particle tracking velocimetry in turbulent flow research using image sequences', *to be published in, Proc. of ISPRS Intercommission Workshop 'From Pixels to Sequences', Zurich, March 22 - 24. In Int'l Arch. of Photog. and Rem. Sens., Vol 30, Part 5W1*

[11] Wierzimok, D., Hering, F.: 1993, 'Quantitative Imaging of Transport in Fluids with Digital Particle Tracking Velocimetry', *Imaging in Transport Processes, Begell House, 297-308*

[12] Wierzimok, D., Jähne, B.: 1991, 'Measurement of wave-induced turbulent flow structures using image sequence analysis', *2nd Int. Symp. Gas Transfer at Water Surfaces, Minneapolis 1990, Am. Soc. Civ. Eng.*